Original Article

DOI: 10.5582/irdr.218.01038

Establishment of a human trisomy 18 induced pluripotent stem cell line from amniotic fluid cells

Kaixuan Xing[1,2], Yazhou Cui[2], Jing Luan[2], Xiaoyan Zhou[2], Liang Shi[2], Jinxiang Han[1,2,*]

[1] *School of Medicine and Life Sciences, University of Jinan-Shandong Academy of Medical Science, Ji'nan, China;*
[2] *Key Laboratory for Rare Disease Research of Shandong Province, Key Laboratory for Biotech Drugs of the Ministry of Health, Shandong Medical Biotechnological Center, Shandong Academy of Medical Sciences, Ji'nan, China.*

Summary **Trisomy 18 (18T) is the second most common autosomal trisomy syndrome in humans, but the detailed mechanism of its pathology remains unclear due to the lack of appropriate models of this disease. To resolve this problem, the current study reprogrammed human 18T amniotic fluid cells (AFCs) into an induced pluripotent stem cell (iPSC) line by introducing integration-free episomal vectors carrying pCXLE-hOCT3/4-shp53-F, pCXLE-hSK, pCXLE-hUL, and pCXWB-EBNA1. The pluripotency of 18T-iPSCs was subsequently validated by alkaline phosphatase staining, detection of iPSC biomarkers using real-time PCR and flow cytometry, detection of embryoid body (EB) formation, and detection of *in vivo* teratoma formation. Moreover, this study also investigated the transcriptomic profiles of 18T-iPSCs using RNA sequencing, and several gene clusters associated with the clinical manifestations of 18T were identified. In summary, the generated induced pluripotent stem cells line has typical pluripotency characteristics and can provide a useful tool with which to understand the development of 18T.**

Keywords: Trisomy 18, induced pluripotent stem cells, disease model, rare disease

1. Introduction

Trisomy 18 syndrome (18T, also Edwards syndrome) is the second most frequent autosomal trisomy syndrome in humans. This syndrome involves the presence of an extra chromosome 18 (*1*). The incidence of 18T is estimated to be 1/6,000-1/8,000 births (*2*). This trisomy usually manifests as abnormal development of multiple tissues and organs during prenatal ultrasound screening and is subsequently confirmed by karyotype analysis of cultured amniotic fluid cells (AFC). As a result of recent developments in and clinical use of next-generation sequencing (NGS)-based noninvasive prenatal diagnosis (NIPD) technologies, an unprecedentedly large number of fetuses with 18T have been screened, and 18T has been identified as a leading cause of miscarriages (*3-5*).

Typically, 18T is characterized by significant growth delay, dolichocephaly, specific facies, limb anomalies, and visceral malformations (*2*). Chromosome 18 has the lowest gene density among human chromosomes (*6*). Unlike other trisomy syndromes such as trisomy 21, knowledge about the pathology and molecular mechanisms of 18T is very limited (*7,8*). This may be partly due to the lack of disease-associated samples and disease models as a result of the syndrome's rareness and extremely high mortality rate (*2,9*).

The recent development of induced somatic cell reprogramming efficiently provides induced pluripotent stem cells (iPSCs) from nearly all types of patient-derived somatic cells, allowing researchers to mimic pathological processes by differentiating iPSCs into disease-associated cells. This can provide novel clues to better understand the biological characteristics of many rare diseases such as 18T. A previous study attempted to establish 18T-iPSCs (*10*). Although

Released online in J-STAGE as advance publication May 15, 2018.

**Address correspondence to:*
Dr. Jinxiang Han, Key Laboratory for Rare Disease Research of Shandong Province, Key Laboratory for Biotech Drugs of the Ministry of Health, Shandong Medical Biotechnological Center, Shandong Academy of Medical Sciences, Ji'nan, Shandong 250062, China.
E-mail: jxhan9888@aliyun.com

pluripotent marker genes were expressed and exhibited pluripotency, the iPSC-like cells lost the extra chromosomes and converted to diploid cells after 10 passages.

To the extent known, the current study is the first to establish typical 18T-iPSCs that exhibited stable pluripotency and trisomy. These 18T-iPSCs exhibited expression profiles that differed significantly from those of normal AFC-derived iPSCs, suggesting new clues to understanding the mechanisms of 18T in embryo and disease development.

2. Materials and Methods

2.1. *AFC sampling and ethnical approval*

Ten-mL AFC samples were obtained from a pregnant woman who underwent an amniocentesis for prenatal diagnosis at Zibo Maternal and Child Health Hospital in Zibo, Shandong, China. Samples were obtained with the woman's informed consent. 18T was diagnosed after chromosomal microarray analysis. The study protocol has been reviewed and approved by the ethics committee of the Shandong Medical Biotechnological Center, Jinan, Shandong, China. After collection, AFC samples were centrifuged at 200 g for 5 minutes at room temperature, and then the cells were washed and cultured with BIOAMF-2 complete medium (Biological, Inc., Kibbutz Beit Haemek, Israel) at 37℃ in a 5% CO_2 atmosphere.

2.2. *iPSC reprogramming and culture*

iPSCs were generated using the procedure that was previously reported (*11-13*). Briefly, 2×10^6 AFC cells were transfected with the plasmids pCXLE-hOCT3/4-shp53-F, pCXLE-hSK, pCXLE-hUL, and pCXWB-EBNA1 (kindly provided by Dr. Fabin Han of Liaocheng People's Hospital, Liaocheng, Shandong, China) through electrotransfection (Lonza Nucleofector and Nucleofector Kit V, Lonza, USA). On day 5 post-transduction, BIOAMF-2 culture medium was changed to iM1 (Osinglay, China). Medium was then replenished every day for 3 weeks, and medium was then changed to BioCISO (Osinglay, China) until uniform colonies were generated. The iPSC colonies were collected on day 26.

2.3. *Characterization of iPSCs using alkaline phosphatase staining, karyotyping, and detection of pluripotency markers*

Alkaline phosphatase staining was performed using the BCIP/NBT Kit (CoWin Biosciences, China) after treatment with 4% polyoxymethylene. Karyotyping of 18T-iPSCs was performed as described previously, and the Metafer karyotyping system (Carl Zeiss AG, Jena, Germany) was used to analyze images. The level of expression of the pluripotency biomarkers NANOG, SOX2, and OCT3/4 in 18T-iPSCs and derived AFCs was compared using real-time PCR. The primers used are listed in Table 1. After dissociation *via* 0.5-μM EDTA digestion and fixation, flow cytometry analysis was used to examine human pluripotency markers with the following antibodies: anti-Oct4 (BD Biosciences, USA), anti-SSEA4 (BD Biosciences, USA), anti-Tra-1-60 (BD Biosciences, USA), and anti-Tra-1-81 (BD Biosciences, USA). Flow cytometry was performed using the BD FACS Aria flow cytometer (BD Biosciences, USA).

2.4. *Embryoid body (EB) formation assay*

For an *in vitro* embryoid body (EB) formation assay, 18T-iPSCs were scraped from plates after dissociation using BioC-PDE1 (Osinglay, China) and cultured in 6-well suspension culture plates with BioCISO-EB1 medium (Osinglay, China) for 7 days to obtain EBs. The EBs were then cultured in 6-well culture plates coated with Matrigel for 7 to 14 days. Cells were then collected, and expression profiles of marker genes in the three germ layers were determined using real-time PCR. Corresponding genes and their primers are listed in Table 1.

2.5. *Teratoma formation assay*

For an *in vivo* teratoma formation, iPSCs were cultured to approximately 85% confluence. After 10-15 minutes of dissociation using Bio-PDE1, cells were scraped from the plates. One hundred and thirty μl of culture medium, 70 μL of Matrigel, and the cell suspension were subcutaneously injected into NOD/SCID mice. After 4-6 weeks, mice were sacrificed, and tumors that developed were fixed in formalin for 24 h and then embedded in paraffin. The specimens were stained with hematoxylin and eosin.

2.6. *Transcriptomic profiles according to RNA sequencing*

The global gene expression profiles of 18T-iPSCs and two normal iPSC lines established from ATCs by this Laboratory were analyzed using RNA-Seq technology. Briefly, total RNA was extracted using the TRIzol reagent (Invitrogen), a library was constructed, and RNA was sequenced with the Illumina HiseqX platform (illumine, USA). RNA sequencing data were expressed as fragments per kilobase of exon per million fragments mapped (FPKM). The Benjamini–Hochberg false discovery rate (FDR) threshold ≤ 0.05 and log2 fold change ≤ -1 or ≥ 1 based on DESeq-normalized read counts were used as criteria to determine differentially expressed genes.

Table 1. List of primers for pluripotency and differentiation markers

Target genes		Primer sequence
OCT4	Forward	CCTCACTTCACTGCACTGTA
	Reverse	CAGGTTTTCTTTCCCTAGCT
SOX2	Forward	CCCAGCAGACTTCACATGT
	Reverse	CCTCCCATTTCCCTCGTTTT
NANOG	Forward	AAGGTCCCGGTCAAGAAACAG
	Reverse	CTTCTGCGTCACACCATTGC
Actin	Forward	CCCAGAGCAAGAGAGG
	Reverse	GTCCAGACGCAGGATG
FOXA2	Forward	CCAACCCCACAAAATGGA
	Reverse	ATAATGGGCCGGGAGTACA
SOX17	Forward	ACCGCACGGAATTTGAAC
	Reverse	GCAGTAATATACCGCGGAGC
BRACHYURY	Forward	CCCTATGCTCATCGGAACA
	Reverse	TTCCAAGGCTGGACCAAT
MSX1	Forward	TCCGCAAACACAAGACGA
	Reverse	ACTGCTTCTGGCGGAACTT
MAP2	Forward	TGAAGCAAAGGCACCTCAC
	Reverse	TATGGGAATCCATTGGCG
PAX6	Forward	TTGCTTGGGAAATCCGAG
	Reverse	TGCCCGTTCAACATCCTT
GAPDH	Forward	GGTGGTCTCCTCTGACTTC
	Reverse	CTCTTCCTCTTGTGCTCTTG

3. Results

The induction of iPSCs from 18T-derived AFCs is summarized in Figures 1A. Figure 1B-1D shows the characteristic morphological changes during iPSC induction from AFCs. At 26-32 days of induction, the 18T-iPSCs were purified and exhibited typical phenotypes like embryonic stem (ES) cells (Figure 1D).

After 18 passages, the 18T-iPSCs exhibited stable 18T karyotypes (Figure 1E). Alkaline phosphatase-positive ES cell-like colonies of 18T-iPSCs were noted (Figure 1F), and real-time PCR and flow cytometry staining revealed significant expression of pluripotent markers (Figures 1F-G). In addition, the generated 18T-iPSCs were found to have differentiated into all three germ layers according to the *in vitro* EB formation assay and the *in vivo* teratoma formation assay (Figure 2D). Taken together, these findings indicate that the established 18T-iPS cell line has obvious pluripotency while maintaining trisomy.

RNA-seq was used to analyze the transcriptomic profile of the 18T-iPSCs in comparison to that of normal AFC-derived iPSCs, and a list of significantly differentially expressed genes was identified (Table 2, Figure 3). Interestingly, a series of genes associated with organ differentiation (the brain, testis cryptorchidism, heart, skin, kidneys, esophagus, bone, and lungs) was found to be differently expressed in 18T-iPSCs compared to normal iPSCs, and these differences in expression may partly account for the comprehensive malformations caused by 18T.

4. Discussion

The current study successfully generated an iPSC line from 18T AFCs. Findings indicated that these 18T-iPSCs were alkaline phosphatase-positive and significantly expressed pluripotency biomarkers such as NANOG, SOX2, OCT3/4, and SSEA4. As further corroboration, these 18T-iPSCs have the potential to differentiate into three germ layers both *in vitro* and *in vivo*. Unlike the 18T-iPS cell line established by Li *et al*. (*10*), the current cell line exhibited stable trisomy after numerous passages. Therefore, the 18T-iPSCs generated in the current study are more representative of 18T.

The current study also observed the genomic instability of 18T-iPSCs in another iPSC line derived from the same AFCs with 18T pregnancies. Although those cells exhibited pluripotency, they spontaneously gained an extra chromosome 8 after more than 10 passages. The current findings confirmed the contention that 18T cells are prone to spontaneously differentiating, but they have built upon results of previous studies by revealing an extra trisomy mutation. Therefore, whether the 18T-iPSCs established here would exhibit genomic instability after more passages is a question that warrants study.

18T is an aberrantly differentiated condition with complicated malformations, and the exact molecular mechanism by which an extra 18 chromosome causes that pathology is not clear (*10*). Interestingly, the current transcriptomic findings indicated that the gene expression of 18T-iPSCs varied significantly from that in normal iPSCs, but the genes in question were not limited to those located on chromosome 18. Moreover, differentiation-associated genes were markedly dysregulated in 18T-iPSCs, suggesting that 18T may involve an aberrant genetic background in the ES cell stage.

In conclusion, this study successfully established a representative 18T-iPSC clone, and it described the molecular characteristics of that clone at the transcriptomic level for the first time. These findings should provide more information with which to understand the pathology of 18T. This 18T-iPSC clone also provides a useful tool with which to study aberrant multi-lineage differentiation in 18T.

Acknowledgements

This work was supported by a grant from the Innovation Project of the Shandong Academy of Medical Science.

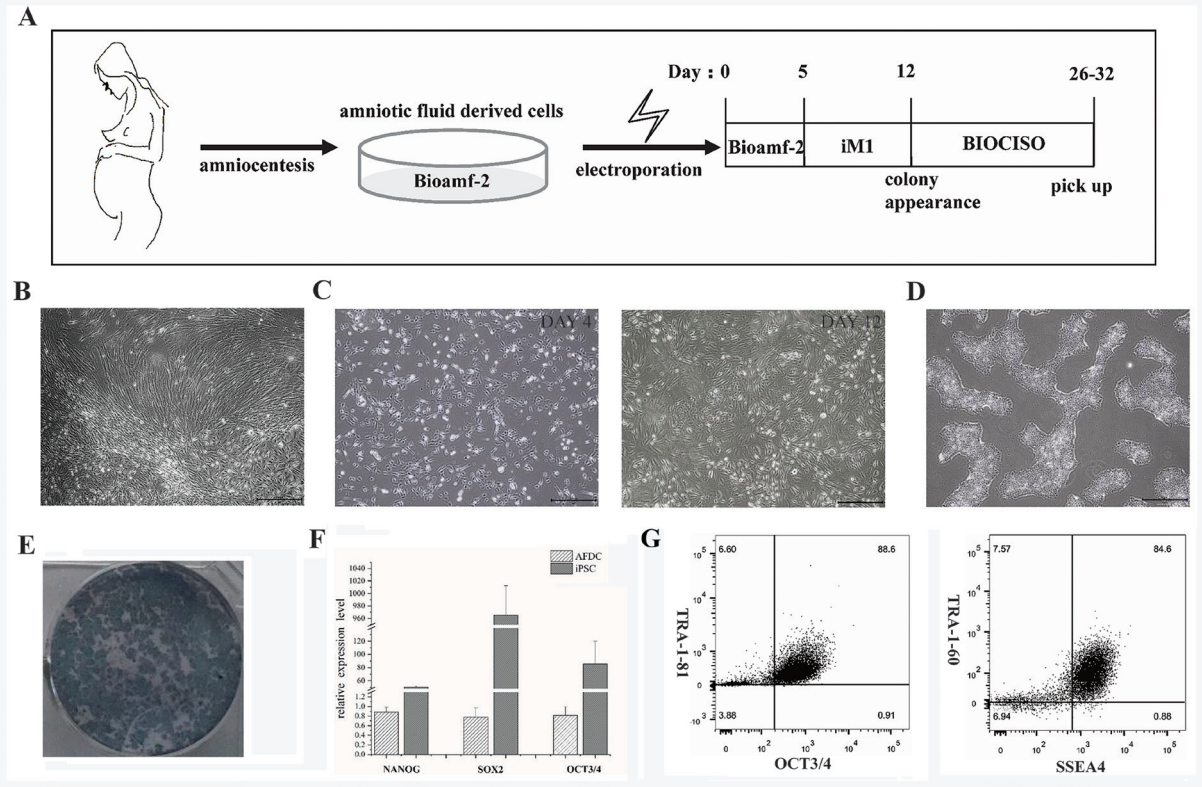

Figure 1. Induction and characterization of 18T-iPSCs from AFC. (A) Timing of iPSCs induction; **(B)** representative images of cells from amniotic fluid cells; **(C)** Day 4 and 12; **(D)** Purified 18T-iPSCs (Scale bar = 500 μm); **(E)** alkaline phosphatase staining; **(F)** Pluripotency biomarkers of 18T-iPSCs detected with real-time PCR and **(G)** flow cytometry.

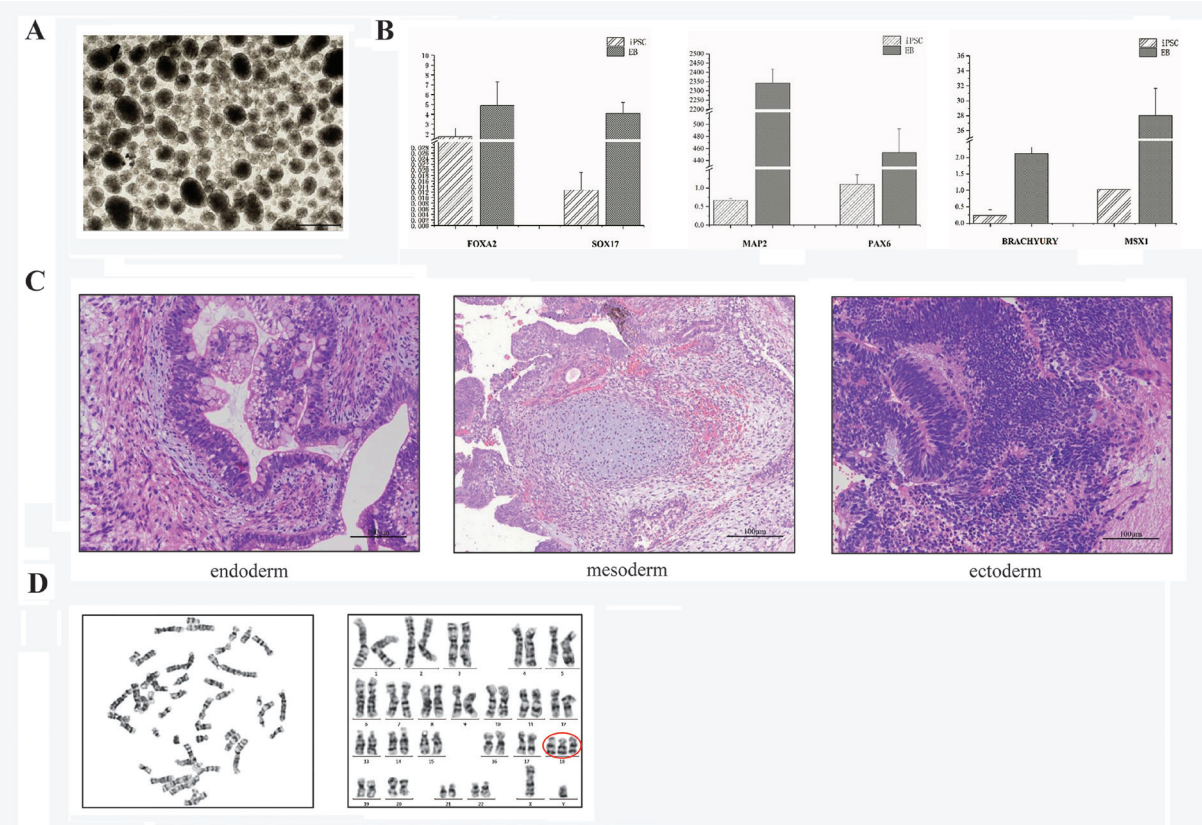

Figure 2. Confirmation of the differentiation potential and trisomy of 18T-iPSC. (A) Embryoid body (EB) formation by 18T-iPSCs (Scale bar = 500 μm); **(B)** Detection of EB biomarkers with real-time PCR; **(C)** Hematoxylin and eosin staining of teratoma derived from a 18T-iPSC clone (Scale bar = 100 μm); **(D)** Karyotype analysis in G-band staining of 18T-iPSCs; chromosome 18 is circled in red.

Table 2. List of significantly differentially expressed genes

Gene ID	Gene symbol	Regulation and expression	
ENSG00000087250	MT3	down	Biased expression in the brain (RPKM 149.3) and adrenal glands (RPKM 10.1)
ENSG00000111262	KCNA1	down	Biased expression in the brain (RPKM 6.1) and thyroid (RPKM 0.3)
ENSG00000151952	TMEM132D	down	Biased expression in the brain (RPKM 5.0) and testes (RPKM 0.4)
ENSG00000105376	ICAM5	down	Biased expression in the brain (RPKM 11.7), lungs (RPKM 3.3), and 1 other type of tissue
ENSG00000196990	FAM163B	down	Biased expression in the brain (RPKM 9.7) and adrenal glands (RPKM 1.9)
ENSG00000143847	PPFIA4	down	Biased expression in the brain (RPKM 8.9), heart (RPKM 8.4), and 10 other types of tissue
ENSG00000136928	GABBR2	down	Restricted expression in the brain (RPKM 33.5)
ENSG00000183775	KCTD16	down	Biased expression in the brain (RPKM 4.6), lungs (RPKM 0.4), and 3 other types of tissue
ENSG00000129990	SYT5	down	Biased expression in the brain (RPKM 20.3) and adrenal glands (RPKM 2.1)
ENSG00000125462	C1orf61	down	Restricted expression in the brain (RPKM 43.3)
ENSG00000141837	CACNA1A	down	Biased expression in the brain (RPKM 5.1), stomach (RPKM 1.8), and 6 other types of tissue
ENSG00000161082	CELF5	down	Biased expression in the brain (RPKM 14.1), ovaries (RPKM 2.1), and 1 other type of tissue
ENSG00000181418	DDN	down	Biased expression in the brain (RPKM 36.7) and kidneys (RPKM 8.9)
ENSG00000165973	NELL1	down	Biased expression in the brain (RPKM 7.1), kidneys (RPKM 6.6), and 2 other types of tissue
ENSG00000138650	PCDH10	down	Biased expression in the brain (RPKM 21.3), placenta (RPKM 10.2), and 4 other types of tissue
ENSG00000242173	ARHGDIG	down	Biased expression in the brain (RPKM 34.7), duodenum (RPKM 7.8), and 4 other types of tissue
ENSG00000177181	RIMKLA	down	Biased expression in the brain (RPKM 2.6), colon (RPKM 1.6), and 10 other types of tissue
ENSG00000131094	C1QL1	down	Biased expression in the brain (RPKM 10.8), kidneys (RPKM 1.7), and 4 other types of tissue
ENSG00000133019	CHRM3	down	Biased expression in the brain (RPKM 5.0), salivary glands (RPKM 2.4), and 12 other types of tissue
ENSG00000111674	ENO2	down	Biased expression in the brain (RPKM 167.6), adrenal glands (RPKM 26.3), and 9 other types of tissue
ENSG00000105605	CACNG7	down	Restricted expression in the brain (RPKM 18.0)
ENSG00000166342	NETO1	up	Biased expression in the brain (RPKM 5.4) and spleen (RPKM 0.5)
ENSG00000160471	COX6B2	down	Restricted expression in the testes (RPKM 26.9)
ENSG00000151948	GLT1D1	down	Biased expression in the testes (RPKM 6.9), bone marrow (RPKM 6.4), and 9 other types of tissue
ENSG00000175513	TSGA10IP	down	Restricted expression in the testes (RPKM 2.7
ENSG00000204961	PCDHA9	down	Biased expression in the testes (RPKM 14.6), endometrium (RPKM 1.3), and 2 other types of tissue
ENSG00000130270	ATP8B3	down	Biased expression in the testes (RPKM 14.6), endometrium (RPKM 1.3), and 2 other types of tissue
ENSG00000205129	C4orf47	down	Biased expression in the testes (RPKM 3.0), thyroid (RPKM 0.8), and 5 other types of tissue
ENSG00000162039	MEIOB	down	Restricted expression in the testes (RPKM 20.3)
ENSG00000248746	ACTN3	down	Biased expression in the testes (RPKM 1.6), prostate (RPKM 0.6), and 2 other types of tissue
ENSG00000118407	FILIP1	down	Biased expression in the heart (RPKM 16.2), esophagus (RPKM 4.3), and 12 other types of tissue
ENSG00000106631	MYL7	up	Restricted expression in the heart
ENSG00000130226	DPP6	up	Biased expression in the brain (RPKM 22.2), endometrium (RPKM 11.9), and 5 other types of tissue
ENSG00000169035	KLK7	down	Biased expression in the skin (RPKM 68.1) and esophagus (RPKM 25.3); Polymorphisms in this gene may play a role in the development of atopic dermatitis.
ENSG00000182580	EPHB3	down	Broad expression in the skin (RPKM 18.6), stomach (RPKM 10.2), and 15 other types of tissue
ENSG00000129455	KLK8	down	Biased expression in the skin (RPKM 32.0) and esophagus (RPKM 29.8)
ENSG00000143590	EFNA3	down	Biased expression in the skin (RPKM 20.5), esophagus (RPKM 8.1), and 3 other types of tissue
ENSG00000183479	TREX2	up	Biased expression in the skin (RPKM 5.9), spleen (RPKM 0.7), and 5 other types of tissue
ENSG00000164879	CA3	down	Biased expression in the kidneys (RPKM 2.5), brain (RPKM 1.7), and 10 other types of tissue
ENSG00000119715	ESRRB	down	Biased expression in the kidneys (RPKM 4.2), heart (RPKM 1.8), and 2 other types of tissue
ENSG00000095932	SMIM24	down	Biased expression in the kidneys (RPKM 301.3), duodenum (RPKM 292.3), and 4 other types of tissue
ENSG00000161270	NPHS1	down	Biased expression in the kidneys (RPKM 12.8), pancreas (RPKM 3.0), and 1 other type of tissue
ENSG00000167755	KLK6	down	Biased expression in the esophagus (RPKM 23.8), brain (RPKM 23.7), and 4 other types of tissue
ENSG00000135046	ANXA1	up	Biased expression in the esophagus (RPKM 2850.3), bone marrow (RPKM 574.5), and 4 other types of tissue
ENSG00000206073	SERPINB4	up	Biased expression in the esophagus (RPKM 63.1), bladder (RPKM 11.6), and 1 other type of tissue
ENSG00000057149	SERPINB3	up	Restricted expression in the esophagus (RPKM 424.4)
ENSG00000012779	ALOX5	down	Broad expression in bone marrow (RPKM 35.1), the lungs (RPKM 26.8), and 15 other types of tissue
ENSG00000161835	GRASP	down	Broad expression in bone marrow (RPKM 8.3), fat (RPKM 7.8), and 23 other types of tissue
ENSG00000059804	SLC2A3	down	Biased expression in bone marrow (RPKM 183.0), the placenta (RPKM 54.5), and 11 other types of tissue
ENSG00000066926	FECH	up	Broad expression in bone marrow (RPKM 19.5), the kidneys (RPKM 8.4), and 24 other types of tissue
ENSG00000171848	RRM2	up	Biased expression in bone marrow (RPKM 28.1), lymph nodes (RPKM 20.5), and 13 other type of tissue
ENSG00000170561	IRX2	up	Biased expression in the lungs (RPKM 4.6), skin (RPKM 2.8), and 9 other types of tissue
ENSG00000105371	ICAM4	down	Biased expression in the lungs (RPKM 3.3), bone marrow (RPKM 3.1), and 13 other types of tissue
ENSG00000179344	HLA-DQB1	down	Broad expression in the lungs (RPKM 158.2), lymph nodes (RPKM 135.4), and 19 other types of tissue
ENSG00000090339	ICAM1	down	Broad expression in the lungs (RPKM 83.1), bone marrow (RPKM 40.5), and 20 other types of tissue
ENSG00000095383	TBC1D2	down	Broad expression in the lungs (RPKM 7.7), bladder (RPKM 3.8), and 23 other types of tissue

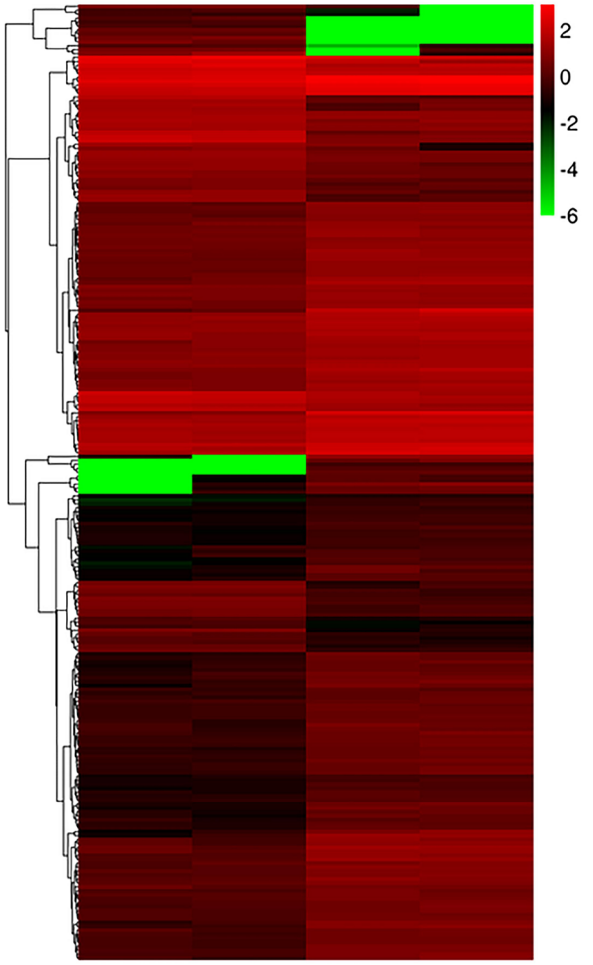

Figure 3. Hierarchical clustering analysis of the differentially expressed genes in 18T-iPSCs and normal karyotype iPSCs. Red indicates upregulated genes and green indicates downregulated genes.

References

1. Edwards JH, Harnden DG, Cameron AH, Crosse VM, Wolff OH. A new trisomic syndrome. Lancet. 1960; 1:787-790.
2. Cereda A, Carey JC. The trisomy 18 syndrome. Orphanet J Rare Dis. 2012; 7:81.
3. Loane M, Morris JK, Addor MC, *et al*. Twenty-year trends in the prevalence of Down syndrome and other trisomies in Europe: Impact of maternal age and prenatal screening. Eur J Hum Genet. 2013; 21:27-33.
4. Stokowski R, Wang E, White K, Batey A, Jacobsson B, Brar H, Balanarasimha M, Hollemon D, Sparks A, Nicolaides K, Musci TJ. Clinical performance of non-invasive prenatal testing (NIPT) using targeted cell-free DNA analysis in maternal plasma with microarrays or next generation sequencing (NGS) is consistent across multiple controlled clinical studies. Prenat Diagn. 2015; 35:1243-1246.
5. Hill M, Wright D, Daley R, *et al*. Evaluation of non-invasive prenatal testing (NIPT) for aneuploidy in an NHS setting: A reliable accurate prenatal non-invasive diagnosis (RAPID) protocol. BMC Pregnancy Childbirth. 2014; 14:229.
6. Nusbaum C, Zody MC, Borowsky ML, *et al*. DNA sequence and analysis of human chromosome 18. Nature. 2005; 437:551-555.
7. Antonarakis SE, Lyle R, Dermitzakis ET, Reymond A, Deutsch S. Chromosome 21 and Down syndrome: From genomics to pathophysiology. Nat Rev Genet. 2004; 5:725-738.
8. Rachidi M, Lopes C. Mental retardation in Down syndrome: From gene dosage imbalance to molecular and cellular mechanisms. Neurosci Res. 2007; 59:349-369.
9. Cavadino A, Morris JK. Revised estimates of the risk of fetal loss following a prenatal diagnosis of trisomy 13 or trisomy 18. Am J Med Genet A. 2017; 173:953-958.
10. Li T, Zhao H, Han X, Yao J, Zhang L, Guo Y, Shao Z, Jin Y, Lai D. The spontaneous differentiation and chromosome loss in iPSCs of human trisomy 18 syndrome. Cell Death Dis. 2017; 8:e3149.
11. Okita K, Matsumura Y, Sato Y, *et a*l. A more efficient method to generate integration-free human iPS cells. Nat Methods. 2011; 8:409-412.
12. Wang L, Chen Y, Guan C, Zhao Z, Li Q, Yang J, Mo J, Wang B, Wu W, Yang X, Song L, Li J. Using low-risk factors to generate non-integrated human induced pluripotent stem cells from urine-derived cells. Stem Cell Res Ther. 2017; 8:245.
13. Li C, Zhou J, Shi G, Ma Y, Yang Y, Gu J, Yu H, Jin S, Wei Z, Chen F, Jin Y. Pluripotency can be rapidly and efficiently induced in human amniotic fluid-derived cells. Hum Mol Genet. 2009; 18:4340-4349.

(Received April 16, 2018; Revised May 11, 2018; Accepted May 12, 2018)